VERSITA
Information Technology and Management Science
doi: 10.2478/itms-2013-0019
2013 / 16

Models of the Monitoring and Control of Natural and Technological Objects

Andrejs Romanovs[1], Arnis Lektauers[2], Oksana Soshko[3], [1-3] *Riga Technical University*, Viacheslav Zelentsov[4], [4] *St.Petersburg Institute for Informatics and Automation of the Russian Academy of Sciences*

***Abstract* – Monitoring of different natural and technological objects is essential in the modern world to ensure a safe and comfortable people's lifestyle; it helps to understand how the planet and its climate change, what role is played by anthropogenic and technological factors in these changes. Different methods and decision-making models are used in the monitoring and control of natural and technological objects; this paper provides an overview of the commonly used models of ground-space monitoring of natural and technological objects, which have been analysed in the framework of the project INFROM.**

***Keywords* – Control, ground-space monitoring, model, natural and technological object**

I. Introduction

The monitoring of natural and technological objects is focused on the issues of changing ecosystems, geosystems, climate and providing services for sustainable economy, healthy environment and better human life by means of the following activities:

- early warning of natural and anthropogenic disasters;
- technologic object security;
- land cover/land change, natural resource usage;
- human health and the preservation of the environment.

This paper presents on-going work on the development of computationally efficient and user-centred geospatial monitoring, analysis and modelling framework that allows processing and integration of remotely sensed data at different spatial and time scales, as well as modelling and simulation for assessment of possible future development scenarios of the monitored and analysed natural and technological objects. The goal is to improve the integrated monitoring and control of cross-border complex natural and technological objects of Latvia and Russia within the INFROM project (Integrated Intelligent Platform for Monitoring the Cross-Border Natural-Technological Systems), ELRI-184 within the Estonia-Latvia-Russia Cross-border Cooperation Programme as a European Neighbourhood and Partnership Instrument 2007–2013.

To develop an integrated technological framework for remote sensing and monitoring of natural and technological systems, it is necessary to classify the objects to be monitored. In general, the objects of natural and technological systems for monitoring and control purposes can be divided into three main classes:

1. environmental and natural resources;
2. objects of technological systems;
3. natural disasters and industrial accidents.

To monitor and forecast ecological objects and processes, different decision-making methodologies and models are used based on land use classification of satellite images, the hydrological data analysis, integration of remote sensing data and hydrological analysis results, etc. This paper provides an overview of the commonly used models of ground-space monitoring of natural and technological objects.

II. Models of Natural Object Monitoring

For monitoring and forecasting, different methodology and decision models are used: land use classification of satellite imagery, hydrologic data analysis, integration of remote sensing images and hydrologic data analysis.

These decision models include microeconomic models, space theory-based models, psychosocial and cognitive models, institution-based models, experience- or preference-based decision models (rules of thumb), participatory agent-based modelling, empirical or heuristic rules, evolutionary programming, and assumption and/or calibration-based rules.

The quality and safety of human life is of high important in the contemporary world and that is why special attention has been devoted to natural disasters:

- flood mapping systems;
- wildfire monitoring systems.

The second field of natural and ecological systems is related to land use:

- land use monitoring systems.

Detection of coastline changes and forest land cover changes is less operational, but a more strategic issue:

- automatic detection of coastline changes;
- forest land cover changes.

A. Disaster Management Model

In this model [1], different remote sensing techniques were mentioned for the monitoring and analyses of such natural disasters as earthquakes, volcanic eruptions, tsunamis, hurricanes, destructive cyclones, landslides, floods. In the current research, an attempt has been undertaken to adapt these remote sensing techniques to geographic information systems, web technologies.

Methodology – land use classification of satellite imagery, hydrologic data analysis, integration of remote sensing images and hydrologic data analysis.

Land use classification of satellite imagery used in this model, minimum distance method:

$$SD_{xyc} = \sqrt{\sum_{i=1}^{n} (\mu_{ci} - X_{xyi})^2} \quad , \qquad (1)$$

where n = the number of bands (dimensions); i= a particular band; c = a particular class; X_{xyi}= the data file value of pixel x,y_{in} band I; μ_{ci}= the mean of data file values in band i for the sample for class c and SD_{xyc}= the spectral distance from pixel x,y to the mean of class c.

Model, maximum likelihood method:

$$P(x|C_i) = \frac{P(x|C_i)P(C_i)}{P(x)} \quad , \qquad (2)$$

where P (x|Ci) – the class probability density; P (Ci) – the prior probability and P (x) – the feature probability density (class-independent).

B. Flood Mapping Models

The authors of flood management model [2] proposed a new GIS-based decision support system developed for integrated flood management within the framework of ArcGIS, based on realistic two dimensional flood simulations. This system has the ability to interact and use classified Remote Sensing image layers and other GIS feature layers, such as zoning layer, survey database and census block boundaries for flood damage calculations and loss of life estimations.

For instance, the equation for retrieving the life loss of a subcategory layer, which satisfies a medium flood severity with no warning time in the domain, is as follows:

$$[LossLife] = \left(([D] < H_{high}) \& ([D] \geq H_{low})\right) \& \left(([AT] - W_{issue}) < W_{nw}\right) \times [Cs] \times R_f \quad ,(3)$$

where *LossLife*, *D*, *AT* and *Cs* represent a raster layer of loss of life, flood depth, arrival time and census block information, respectively, H_{high}/H_{low} are the limits for high/low severity flood depth, W issue is the initial time of a public warning, W_{nw} is the time limit for no warning, and R_f is the corresponding fatality rate.

An automated SAR-based flood monitoring system model introduces two variants of an automated SAR-based flood extraction algorithm with and without integration of pre- or post-flood reference images.

Spaceborne SAR data have proven to be efficient tools not only in flood monitoring, but also in flood forecasting through near real-time assimilation of remote sensing-derived flood extent data in coupled hydrologic–hydraulic models.

The method proposed in the current research is composed of three processing stages:

- estimation of the statistical distribution of 'water' backscatter values from the SAR flood image:

$$f_{\sigma^0_m}\left(\frac{\sigma^0}{k}\right) = \frac{[(\sigma]^0 - \sigma^0_1)^{k-1}}{\left(\frac{(\sigma^0_m - \sigma^0_1)}{k-1}\right)^k \Gamma(k)} e^{-\frac{[(\sigma^0_1 - \sigma^0_1)(k-1)}{(\sigma^0_m - \sigma^0_1)}} \quad , \qquad (4)$$

- radiometric threshold of the SAR image in order to extract the core of the water bodies;
- region growing to extract all water bodies.

C. Wildfire Monitoring Models

In the fire risk assessment model [3] an integration framework for fire risk evaluation was proposed. The system was based on two groups of factors: those associated to the probability that a fire occurs (Modelling the human factors of fire ignition, Ignition potential from lightning, Ignition potential associated with fuel moisture content status) and those related to the potential damages of fires (Propagation potential, Socioeconomic values, Degradation potential, Landscape value).

Based on this model, the conceptual scheme for fire risk assessment was defined, and the methods used to generate the risk parameters were described.

Once the overall production for acorns was estimated, the potential damage of losing those resources by a forest fire was computed as follows:

$$V = \frac{PR\left((1+i)^{(T-e)} - 1\right)}{i(1+i)^{(T-e)}} \quad , \qquad (5)$$

where V is the assessment of potential losses, P – the production of acorns (kg ha−1), R – the price (€kg−1), i – the annual depreciation, T – the rotation for the oaks (in years) and e is the age of the species for the year of the fire (in years).

D. Detection of Coastline Change Models

The methodology developed in the automatic detection of shoreline change model [4] consists of the automatic delineating of the land/sea boundary using segmentation algorithms that evaluate TOA (Top of the Atmosphere) reflectance of Landsat satellite images. Also for the coastline delineation for coastal wetlands the NDWI index and automatic threshold technique by Otsu (1979) and Sezgin and Sankur (2004) for TM Bands (4 and 2) and Landsat Enhanced Thematic Mapper Plus (ETMþ) are used.

In this model, coastlines were extracted from satellite images for 1972, 1984, 1987, 1998, 2002 and 2009 by segmentation with a histogram based on the automatic threshold method. The coastline rate of change was calculated using DSAS software and two different statistical techniques: End Point Rate (EPR) and Linear Regression Rate-of-Change (WLR).

Based on this model, a new approach was proposed in the conceptual level using a flowchart of the automatic coastline extraction methodology.

Storm impact model along European coastlines [5], [6] is based on results from two projects on marine storm impact along European coastlines. These two projects focus on different purposes, one project concentrates on the physical aspects of the problem (MICORE) and the other one on the socioeconomic implications (ConHaz).

The MICORE Project (16 partners from 9 European countries) aims to provide on-line predictions of storm-related physical hazards, hydrodynamic and morphodynamic impacts. The ConHaz Project addresses the socioeconomic implications that should actually materialize these (or other) hazards.

The methodology in this model is suggested by the FP VI Flood-site Project and the schematic approach adopted by FEMA in the USA.

In these projects for morphological modelling, the modelling techniques were used, which were based on an open source approach using the XBeach model.

The total wave energy dissipation, i.e., directionally integrated, due to wave breaking is modelled according to Roelvink:

$$\bar{D}_w = 2\frac{\alpha}{T_{rep}} Q_b E_w \,,$$

$$Q_b 1 - \exp\left(-\left(\frac{H_{rms}}{H_{\max}}\right)^n\right), H = \sqrt{\frac{8E_w}{\rho g}}, H_{max} = \frac{\gamma \tanh kh}{k} \quad (6)$$

On the model of long-term morphological evolution of Darss–Zingst peninsula, at the southern Baltic Sea coast (1900–2000), coastline changes were simulated with different grid resolutions [7].

Simulation of the decadal-to-centennial morphological evolution of the Darss–Zingst peninsula is based on a multi-scale process-based model consisting of eight main modules to calculate different physical processes that drive the evolution of the specific coastal environment.

The model consists of 8 modules:

1) A 2DH (two-dimensional vertically integrated) circulation module:

$$\frac{\partial \eta}{\partial t} + \frac{\partial (UD)}{\partial x} + \frac{\partial (VD)}{\partial y} = 0 \,,$$

$$\frac{\partial U}{\partial t} + U\frac{\partial U}{\partial x} + V\frac{\partial U}{\partial y} - fV = -g\frac{\partial \eta}{\partial x} + g\frac{(\tau_{ax} - \tau_{bx})}{\rho D} + \frac{F_x}{D} + \upsilon\left(\frac{\partial^2 U}{\partial x^2} + \frac{\partial^2 U}{\partial y^2}\right)$$

$$\frac{\partial V}{\partial t} + U\frac{\partial V}{\partial x} + V\frac{\partial V}{\partial y} - fU = -g\frac{\partial \eta}{\partial y} + g\frac{(\tau_{ay} - \tau_{by})}{\rho D} + \frac{F_y}{D} + \upsilon\left(\frac{\partial^2 V}{\partial x^2} + \frac{\partial^2 V}{\partial y^2}\right) \quad (7)$$

where η is the free water surface, U, V are the flow velocity along x and y direction, respectively. D is the water depth defined as D ¼ H þ h, where H is the static water depth. P is the average water density, g is gravitation acceleration, f is the Coriolis coefficient. τox, τoy represent the surface wind stress calculated by the wind-induced wave module; τbx, τby represent the bottom stress calculated by the bottom boundary module; u is the eddy viscosity coefficient. Fx and Fy are the gradient terms of radiation stresses resulting from wave breaking.

2) A wind-induced wave module calculating wave parameters for nearshore currents and bottom shear stress.

3) A bottom boundary layer (BBL) module calculating the bottom shear stress generated by the combined effects of currents and waves.

4) A sediment transport module calculating sediment fluxes:

$$\frac{\partial DC}{\partial t} + \frac{\partial DuC}{\partial x} + \frac{\partial DvC}{\partial y} + De - Er - \varphi_{source} = \frac{\partial}{\partial x}\left(DA_h \frac{\partial C}{\partial x}\right) + \frac{\partial}{\partial y}\left(DA_h \frac{\partial C}{\partial y}\right), \quad (8)$$

where C is the suspended sediment concentration; De represents deposition flux and Er represents resuspension flux. Calculation of these two parameters follows the framework of ECOMSED. The horizontal eddy diffusivity (Ah) is calculated using the Smagorinsky eddy parameterization. The term φ-source denotes the sediment source term from the lateral boundary (by erosion of the cliff and sandy beach):

$$\varphi_{source} = \begin{cases} 0, \text{for non} - \text{for lateral boundary cells} \\ \varphi_{lateral}, \text{for lateral boundary cells} \end{cases} \quad (9)$$

5) A cliff erosion module calculating the lateral sediment fluxes from the cliff and the beach elements:

$$R' = \begin{cases} \frac{K}{T'} ln\left(\frac{F_w}{F_r}\right), F_w > F_r, \\ 0, F_w \le F_r \end{cases} \quad (10)$$

where R0 is the erosion rate within one wave-period (m/s); Fr is the mechanical strength of the cliff (MPa); Fw is the destructive force of the waves (MPa) given by:

$$F_w = \sin\theta \left(\frac{\rho g H^2}{8}\right) C_n, \quad (11)$$

where θ is the angle between the direction of wave propagation and the wall of the cliff. H is the significant wave height at the base of the cliff; C_n is the group velocity of the waves. Values of these parameters are provided by the wave module.

The eroded material from the cliff serves as the source term for the sediment transport equation, which is given by:

$$\varphi_{source} = \begin{cases} f_{coh} \frac{R' \Delta x H_{cliff}}{T_{wave}}, \text{for silt/clay} \\ (1 - f_{coh}) \frac{R' \Delta x H_{cliff}}{T_{wave}}, \text{for sand} \end{cases} \quad (12)$$

where Δx is the grid cell width at the cliff; Hcliff is the cliff height; fcoh is the fraction of cohesive sediment of the eroded material. fcoh=0.7 is assumed for the glacial till cliff elements and 0.1 – for 'dune cliff' elements.

6) A nearshore storm module calculating the sand-dune erosion, overwash and breaching under extreme wind conditions, bathymetry update is given by:

$$\Delta H_{n+1} = mf \times \left(\sum_{k=1}^{M} \Delta\lambda_k \Delta z_k - \Delta D_{n+1} + \Delta E_{n+1} + \Delta SL_{n+1} \Delta\gamma_{n+1} + f_s \Delta z^s \right), \quad (13)$$

where ΔHn+1 is the bed elevation change during the (n+1)th cycle of hydrodynamic computation; mf is a morphological update factor; Δzk is the thickness of that layer of the condensable sediment ($1 \leq k \leq M$, where M is the user-defined number of condensable sediment layers above the marine base); ΔDn+1 and ΔEn+1 are the thickness of sediment deposition and erosion in the (n+1) cycle of model run calculated from the representative yearly wind series, respectively; ΔSLn+1 is the sea-level change for the (n+1)th cycle of computation; Δγn+1 represents the corresponding geotectonic movement; fs is the frequency of a representative north-easterly storm and Δzs is the calculated storm-induced bathymetrical change; Λk is the long-term compaction rate for the kth layer of the condensable sediment.

7) A bathymetry update module calculating the long-term bathymetric change, and

8) A long-term control function set up-scaling the processes from the short term to the long term.

E. Forest Land Cover Changes

In risk assessment of wind damage in forest management model [8] a GIS-based decision support system (DSS) was built for assessing the risk of wind damage by integrating a forest growth and yield model SIMA and a mechanistic wind damage model HWIND into GIS software ArcGIS 8.2. ArcObjects in ArcGIS and Microsoft Visual Basic 6 were used to develop the Windows-based system. The HWIND model was issued in this DSS to describe the mechanistic behaviour of Scots pine, Norway spruce and birch trees (pure stands) under wind loading.

This DSS can help forest managers to analyse and visualize (charts, maps) the possible effects of forest management, such as clear-cuts, on both the immediate and long-term risks of wind damage at both stand and regional levels.

The total mean wind-induced force is the sum of the wind forces acting at each point on the stem and crown (F1), which is given at height z by:

$$F_1(z) = \frac{1}{2} C_d \rho u(z)^2 A(z), \quad (14)$$

where u is the mean wind speed (ms−1), A (m2) is the streamlined projected area of the stem and crown against which the wind acts, Cd is the drag coefficient and ρ (kg m−3) is the density of the air.

F. Land Use Monitoring Models

In spatial and multi-level models of tropical land use and cover change model [9], Geographically Weighted Regression was applied and compared to multi-level models. Together, these models can draw a more complete picture of land cover change patterns in Guatemala and elaborate more comprehensive implications for theory, empiricism, and policy.

Data used for this analysis come from three sources: 2000 Guatemalan Living Standards Measurement Survey, 2003 Guatemala National Agriculture Census, and 2001–2009 Forest Cover Change database for all municipalities in Latin America. The three data sources provide detailed information regarding land.

In this model the following approach are used: multi-level/grouped models and spatial analysis and modelling.

The GWR (Geographically Weighted Regression) for this study is stated as follows:

$$\gamma_i = \beta_{i0} + \sum_{k=1}^{n} \beta_{ik} x_{ik} + \varepsilon_i, \quad (15)$$

where βi0 is the intercept at location i with latitude and longitude coordinates that correspond to the centroid of each municipality and department, n is the number of model independent variables, and βik is a value of βk at point i. For this model yi is the percentage of land identified by satellite imagery as forest cover in 2009 in the first model, and the change in forest cover from 2001 to 2009 in the second model. βk is regression parameter estimates with corresponding explanatory variables xk, with independent error term ε at location i.

The two-level random-intercept linear regression model is written as follows:

$$y_{ij} = \beta_1 + \beta_2 x_{2ij} + \cdots + \beta_p x p_{ij} \beta_2 + \varsigma_j + \varepsilon_{ij}, \quad (16)$$

For the first model, y_{ij} is the percentage of land identified by satellite imagery as woody vegetation in 2009, where i represents municipalities within j departments. For model 2, y_{ij} is the ratio of municipal woody vegetation from 2001 to 2009, where i represents municipalities within j departments. β_1 is the intercept along with its independent error term ς_j while β_2 through β_p are regression coefficients with corresponding explanatory variables $x2_{ij}$ through xp_{ij} with their independent error term ε_{ij}.

In discrimination of vegetation and burned area model [10], a transformation on the near-infrared (NIR) and middle-infrared (MIR) was defined with the aim of enhancing the spectral information in such a way that vegetated surfaces may be effectively discriminated and then ranked according to the water content of vegetation, leading to the distinction between green vegetation and burned surfaces. The purpose of transformation design is to make a synergic use of advantages of indices, like BAI, that rely on the concept of distances to a fixed point and of indices, like NDVI and VI, which incorporate differences between channels. Remotely-sensed observations were gathered over two main Brazilian biomes, namely the Amazon Forest and the Cerrado region as covered by 16 Landsat ETM+ images. Burned Area Index (BAI):

$$BAI3 = \frac{1}{(\rho_{NIR} - \rho_{CNIR})^2 + (\rho_{MIR} - \rho_{CMIR})^2}, \quad (17)$$

where ρCNIR and ρCMIR are the coordinates of the above-mentioned convergence point, given by the NIR minimum and MIR maximum values of reflectance for burned vegetation.

GEMI is an optimized vegetation index designed to minimize contamination of the vegetation signal by extraneous factors, such as the atmosphere and the soil background. GEMI was modified by replacing AVHRR channel 1 (R) by channel 3 (MIR) leading to the so-called GEMI3:

$$GEMI3 = \frac{Y(1-0.25\theta)-(\rho_{MIR}-0.125)}{1-\rho_{MIR}},$$
$$where: Y = \frac{1(\rho_{NIR}^2-\rho_{MIR}^2)+1.5\rho_{NIR}+0.5\rho_{MIR}}{\rho_{NIR}+\rho_{MIR}+0.5} \quad (18)$$

New vegetation index, the so-called VI3, which is a modified version of the traditional NDVI:

$$VI3 = \begin{cases} \frac{(\rho_{NIR}-\rho_{MIR})}{(\rho_{NIR}+\rho_{MIR})}, \text{for} \rho_{NIR} \geq \rho_{RED} \\ 0, \text{for} \rho_{NIR} < \rho_{RED} \end{cases}, \quad (19)$$

where ρMIR and ρRED are the MIR and red reflectance, respectively. The restriction ρNIR≥ρRED prevents the index from being erroneously applied to water surfaces, where it is defined.

Cropping system model at a regional scale [11] is based on results from the SEAMLESS project, in which an integrated assessment and modelling platform was developed for carrying out ex-ante policy assessments, like agricultural policies of the European Commission with an aim to improve the sustainability of agriculture in the European Union.

APES is a generic cropping system model that operates at the scale of an individual homogeneous field. This system is composed of two main groups of software units: simulation engine on MODCOM modelling framework and model components (cross-component unit to compute mass balance).

Modelling efficiency (EF) is defined as follows:

$$EF = 1 - \frac{\sum_{i=1}^{n}(Y_i-\hat{Y}_i)^2}{\sum_{i=1}^{n}(Y_i-\overline{Y})^2}, \quad (20)$$

where *Yi* is the observed value in site class i, $\hat{Y}_i$ is the simulated value, $\overline{Y}$ is the average of the observed values and *n* is the total number of site classes.

The aim of the model of global crop production assessments was the assimilation and utilization of NASA Earth Observation System (EOS) data [12]. To achieve the aim set, systematic benchmarking techniques were used to evaluate the effectiveness of risk-reducing mitigations.

NASA's Jet Propulsion Laboratory developed the Defect Detection and Prevention (DDP) risk management software tool. This tool was employed to quantify the effectiveness of the enhancements, using attainment of objectives as performance indicators and risk balance. This support tool assimilates satellite data (e.g., MODIS, ASTER, AMSR).

To understand the impacts that climate variability, landscape change, and anthropogenic and economic forces have on global agricultural production, Earth science data are used. This data, models and geographic information systems in agricultural monitoring and assessment continue to expand our ability to understand the impact on climate, etc.

In this model, a decision support system conceptual model is presented for estimating global crop production from disparate data.

III. Models of Technological Object Monitoring

Technological systems include a variety of objects that are manmade or pertaining to a process or substance created by human technology [13], [14]. Monitoring of technological objects allows observing changes in the object in order to:

- optimize processes related to the object;
- prevent events leading to damage of the object;
- determine areas affected by the operation of the object;
- evaluate financial, ecological or other metrics of the object.

Technical models for monitoring the object are similar to conceptual models of the object and mainly are determined by an objective of monitoring. Thus, it is impossible to describe all possible models and the paper contains several models for the most prioritized issues.

A. Monitoring of Cracks and Bowing in Structural Walls

Analysis of measurements on beams shows that there are several mathematical equations for calculation factors that cause cracks and bowing. For example, to account for the major factors affecting crack width, ACI Committee 224 recommends the following flexural crack-width formula, which is based on the so-called Gergely-Lutz equation:

$$w = 2.2\beta\varepsilon_s\sqrt[3]{d_c A}, \quad (21)$$

where w – the most probable crack width; β – the ratio of distance between the neutral axis and tension face to the distance between the neutral axis and the centroid of reinforcing steel; ε_s – strain in reinforcement due to the applied load; d_c – thickness of cover from tension face to centre of the closest bar (in.); and A – the area of concrete symmetric with respect to reinforced steel divided by the number of bars.

Using this formula, it is possible to follow the probability of cracks in structural walls, for example, by monitoring thickness of covers. In a similar way, it is possible to monitor using other formulas that are found in other studies [15], [16], [17].

B. Monitoring of Soil Undermining by Burst Water Main

Soil liquefaction is a process in which over a very short period of time (several seconds or tens of seconds) during ground shaking, the soil transforms from its normal solid state into a heavy liquid mass [18]. Several monitoring models are described in literature [19-22] for monitoring, which can be performed from land and from the space. One of the models is seen in Fig. 1.

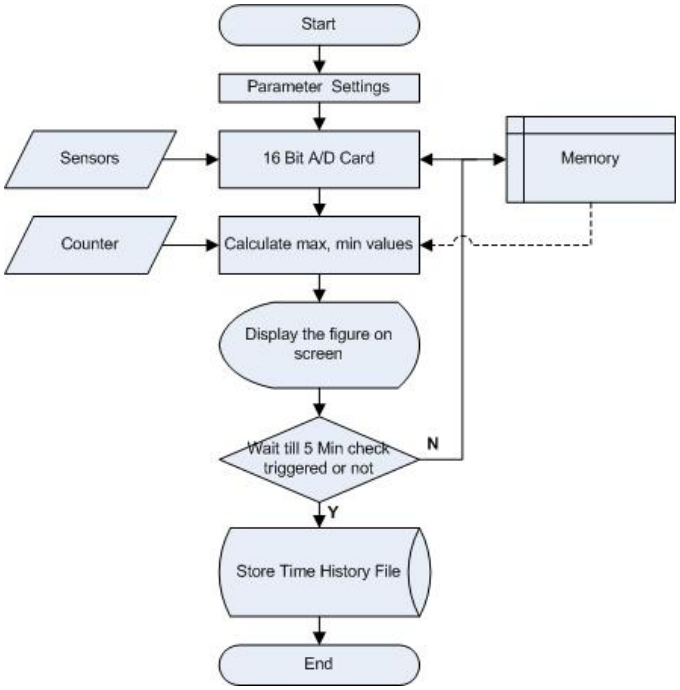

Fig. 1. Flow chart of the monitoring program [9]

C. Calculating the Amount of Available Power for Hydroelectric Power Station

A hydropower resource can be evaluated by its available power [23], [24]. The power available from falling water can be calculated from the flow rate and density of water, the height of fall, and the local acceleration due to gravity. In SI units, the power is:

$$P = \eta \rho Q g h, \tag{22}$$

where P – power in watts; η – the dimensionless efficiency of the turbine; ρ – the density of water in kilograms per cubic meter; Q – the flow in cubic meters per second; g – the acceleration due to gravity; h – the height difference between inlet and outlet.

Parameters that are necessary for calculation of the power can be monitored in order to receive better results [25].

D. Calculating the Amount of Available Power for Wind Farms

Amount of produced power depends on many factors, such as a shape of a propeller, height of constrictions, wind flow etc. Thus, there are many complicated formulas for power calculation [26], [27], [28]. However, they can be simplified to the one:

$$P = \frac{S \rho v^3}{2}, \tag{23}$$

where P – power; S – swept area; ρ – air density; v – velocity.

This formula allows making a monitoring model for calculating the amount of available power for wind farms, where swept area is a constant for specific equipment, air density is calculated using the ideal gas law, expressed as a function of temperature and pressure that can be easily monitored and velocity of wind that can be monitored as well.

E. Road Wear

There are multiple [29-32] papers on the modelling of pavement deterioration and its prevention, including methods like calculation of relative effects of different axle loads or annual change in roughness as seen in (24).

$$\Delta RI = K_{gp}\left[\Delta RI_s + \Delta RI_c + \Delta RI_r + \Delta RI_t\right] + \Delta RI_e, \tag{24}$$

where ΔRI – the total incremental change in roughness during the analysis year, in m/km IRI; Kgp – the calibration factor for roughness progression; ΔRIs – the incremental change in roughness due to structural deterioration during the analysis year, in m/km IRI; ΔRIc – the incremental change in roughness due to cracking during the analysis year, in m/km IRI; ΔRIr – the incremental change in roughness due to rutting during the analysis year, in m/km IRI; ΔRIt – the incremental change in roughness due to potholing during the analysis year, in m/km IRI; ΔRIe – the incremental change in roughness due to an environment during the analysis year, in m/km IRI.

IV. Models of Object Monitoring in Crisis Situations

Crisis situations for NTS systems can be caused by natural disasters or by industrial accidents.

A natural disaster is a major adverse event resulting from the earth's natural hazards. A natural disaster can include loss of life, injury, economic loss, and environmental loss. The severity of the losses depends on the ability of the affected population to resist the hazard, also called their resilience [33]. Natural disasters for project area includes the following:

- earthquakes;
- extreme heat;
- floods;
- severe weather;
- thunderstorms and lightning;
- wildfires;
- winter storms and extreme cold.

Industrial disasters or accidents are disasters caused by industrial companies, either by accident, negligence or incompetence [34]. They are a form of industrial accident, where great damage, injury or losses of life are caused. Other disasters can also be considered industrial disasters, if their causes are rooted in the products or processes of industry. Since there is little or no warning of industrial/chemical accidents, the loss incurred is very high. There is a huge loss to life, property, livelihood and environment. Hazardous materials in various forms can cause death, serious injury, and damage to buildings, homes and other properties. The areas close to an industrial setup are under immediate threat. People working in that industry or people residing in the neighbouring areas are normally affected. Main disasters can be classified in the following industries:

- chemical industry and hazardous materials;
- construction industry;

- energy industry and power outage;
- manufacturing industry.

A. Monitoring of Earthquakes

There is no accepted method to predict earthquakes; however, some regions are more prone to earthquakes than others due to their location in proximately to earthquake faults.

Modern seismographic systems precisely amplify and record ground motion (typically at periods of between 0.1 and 100 seconds) as a function of time. This amplification and recording as a function of time is the source of instrumental amplitude and arrival-time data on near and distant earthquakes. Although similar seismographs have existed since the 1890s, it was only in the 1930s when Charles F. Richter, California seismologist, introduced the concept of earthquake magnitude [35].

Richter's original magnitude scale (ML) was then extended to observations of earthquakes of any distance and of focal depths ranging between 0 and 700 km. Because earthquakes excite both body waves, which travel into and through the Earth, and surface waves, which are constrained to follow the natural wave guide of the Earth's uppermost layers, two magnitude scales evolved – the mb and MS scales.

The standard body-wave magnitude formula is as folows:

$$m_b = \log_{10}(\frac{A}{T}) + Q(D,h), \quad (25)$$

where A – the amplitude of ground motion (in microns); T – the corresponding period (in seconds); Q(D,h) – a correction factor that is a function of distance; D – degrees among the epicentre, an station and focal depth of the earthquake; h – the focal depth of the earthquake (in kilometres).

The standard surface-wave formula is as follows:

$$M_s = \log_{10}(\frac{A}{T}) + 1.66\log_{10}(D) + 3.30, \quad (26)$$

There are many variations of these formulas that take into account effects of specific geographic regions so that the final computed magnitude is reasonably consistent with Richter's original definition of ML.

Description of effects based on a magnitude is given in Table I:

TABLE I

EFFECTS BASED ON MAGNITUDE [35]

Magnitude	Description of effects
Less than 3.4	Usually felt by only a few people near the epicentre
3.5 - 4.2	Felt by people who are indoors and some outdoors, vibrations similar to passing a truck
4.3 - 4.8	Felt by many people, windows rattle, dishes disturbed, standing cars rock
4.9 - 5.4	Felt by everyone, dishes break and doors swing, unstable objects overturn
5.5 - 6.1	Some damage to buildings, plaster cracks, bricks fall, chimneys damaged
6.2 - 6.9	Much building damage, houses move on their foundations, chimneys fall, furniture moves
7.0 - 7.3	Serious damage to buildings, bridges twist, walls fracture, many buildings collapse
7.4 - 7.9	Causes significant damage, most buildings collapse
8.0 and over	Causes extensive damage, waves seen on the ground's surface, objects thrown into the air

B. Extreme Temperatures

Changes in extreme weather and climate events have significant impacts and are among the most serious challenges to society in coping with a changing climate. As a result, the demand for information services on weather and climate extremes is growing. The sustainability of economic development and living conditions depends on our ability to manage the risks associated with extreme events. Models for monitoring temperature are widely recognized and available in literature [36], [37]. One of the models is a wind chill temperature index (WCTI) based on wind chill models. The model used wind, air temperature, and solar radiation as the environmental factors in the wind chill formula:

$$WCTI = 13.12 + 0.3215T - 11.37V^{0.16} + 0.3965TV^{0.16}, \quad (27)$$

where WCTI – the wind chill temperature index; T – the air temperature in °C; V – the wind speed in km h-1 at 10 m elevation.

C. Floods

Space-based river monitoring can provide a systematic, global, timely and impartial way to monitor disastrous floods. This paper describes a methodology to use daily passive microwave observations to detect, map and size floods, both for the purposes of global humanitarian organizations and national hydrological services. Early warning is possible by monitoring upstream areas, with warning lead times up to 30 days. Flood maps are of a low resolution but match maps derived from high-resolution imagery. The interest lies in their daily availability, allowing us to understand the dynamic aspects of floods. Finally, objective flood sizing is achieved by integrating information over time and space [38], [39].

Using Advanced Microwave Scanning Radiometer – Earth Observing System (AMSR-E) data, a method for detecting major floods on a global basis is developed, in a timely and impartial way appropriate for humanitarian response. The methodology uses the brightness temperature at 36.5 GHz H-polarization during the descending (night) orbit of AMSR-E with a footprint size of approximately 8612 km2 and an average revisit time at 1 day. Brightness temperature is related to the physical temperature T and the emissivity e of an object: Tb¼eT. Due to the different thermal inertia and emission properties of land and water, the observed microwave radiation in general accounts for a lower brightness temperature values for water (Tb,water) and higher for land (Tb,land4Tb,water). Since each observation of the satellite (or pixel) covers a relatively large area of 8612 km2, the observed

brightness temperature is mostly composed of both water and land values, in proportion to the relative area of water (w) and land (1 – w) in the pixel.

$$T_b = (1-w)T_{b,land} + wT_{b,water}\,, \qquad (28)$$

where w is the water portion of the pixel.

If the physical temperature remains constant, changes in brightness temperature will be related to changes in water surface extent in the pixel. However, in spite of the great radiation dissimilarity of water and land cover, the raw brightness temperature observations cannot be used to reliably detect changes in surface water area. This is because brightness temperature (Tb) measures are influenced by other factors, such as physical temperature, differences in emissivity and atmospheric moisture. While the relative contribution of these factors cannot be measured, they are assumed to be constant over a larger area. As shown in (2.5), the ratio between two nearby pixel values is a function of w alone. Therefore, by comparing a 'wet pixel' received over a river channel of a potential inundation location (w40) with a 'dry pixel' without water cover (w¼0), the mentioned noise factors can be reduced. The brightness temperature values of the measurement/wet signal are divided by the calibration/dry observations, referred to as M/C ratio or signal s.

$$\begin{aligned} T_{b,measurment} &= (1-w)T_{b,land} + wT_{b,water} = T_{measurment}((1-w)\varepsilon_{land} + w\varepsilon_{water}) \\ T_{b,calibration} &= T_{b,land} = T_{calibration}\varepsilon_{land} \end{aligned}\,, \qquad (29)$$

If, for nearby pixels, we assume

$$\varepsilon_{land,measurment} \approx \varepsilon_{land,calibration} \approx \varepsilon_{land}\,, T_{measurment} \approx T_{calibration}\,, \qquad (30)$$

then

$$s = \frac{M}{C} = \frac{T_{b,measurment}}{T_{b,calibration}} = \frac{T_{measurment}((1-w)\varepsilon_{land} + w\varepsilon_{water})}{T_{calibration}\varepsilon_{land}} \approx 1 - w + w\frac{\varepsilon_{water}}{\varepsilon_{land}} = f(w)\,, \qquad (31)$$

D. Wildfires

Fires, whether of human or natural origin, have profound effects on land cover, land use, production, local economies, global trace gas emissions, and health. Uncontrolled wildfires can have an immense impact on the human population and the environment. A fire analysis cycle can be defined that moves from mapping the potential for a fire start if there is ignition, to detecting the start of a fire, through monitoring the progression of a fire, to mapping the extent of the fire scars and the progression of vegetation regeneration [40]. Such information would be useful to managers, policy makers and scientists interested in mitigating and evaluating the effects of wildfires.

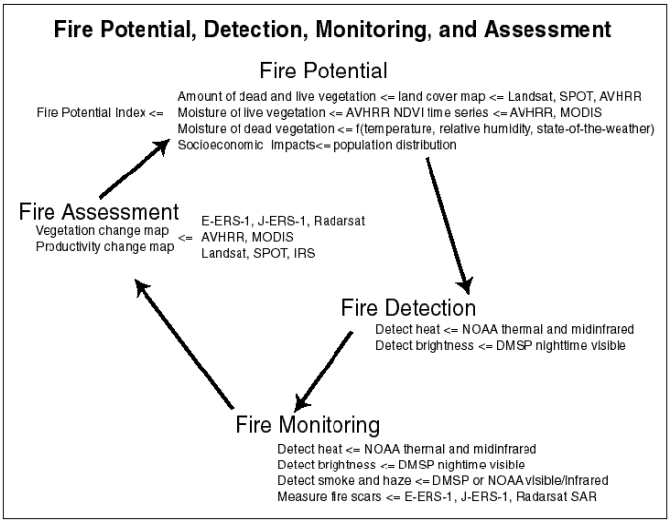

Fig. 2. Fire analysis cycle [40]

E. Hazardous Materials

A hazardous material is defined as any substance or material that could adversely affect the safety of the public, handlers or carriers during transportation [41]. There are nine classes of hazardous materials (see Table II):

TABLE II

CLASSES OF HAZARDOUS MATERIALS [42]

Hazard Class	Material
Hazard Class 1: Explosives	Mass explosion hazard; Projectile hazard; Minor blast/projectile/fire; Minor blast; Insensitive explosives; Very insensitive explosives
Hazard Class 2: Compressed Gases	Flammable gases ; Non-flammable compressed gases; Poisonous gases
Hazard Class 3: Flammable Liquids	Flammable (flash point below 141°C); Combustible (flash point between 141°C-200°C)
Hazard Class 4: Flammable Solids	Flammable solids; Spontaneously combustible; Dangerous when wet
Hazard Class 5: Oxidizers and Organic Peroxides	Oxidizer; Organic Peroxide
Hazard Class 6: Toxic Materials	Material that is poisonous; Infectious Agents
Hazard Class 7: Radioactive Material	Radioactive I; Radioactive II; Radioactive III
Hazard Class 8: Corrosive Material	Destruction of the human skin; Corrode steel at a rate of 0.25 inches per year
Hazard Class 9: Miscellaneous	A material that presents a hazard during shipment but does not meet the definition of the other classes

Hazardous material monitoring depends on the type of material and several models are described in the literature both for risk assessment and for the evaluation of incidents [41, 42].

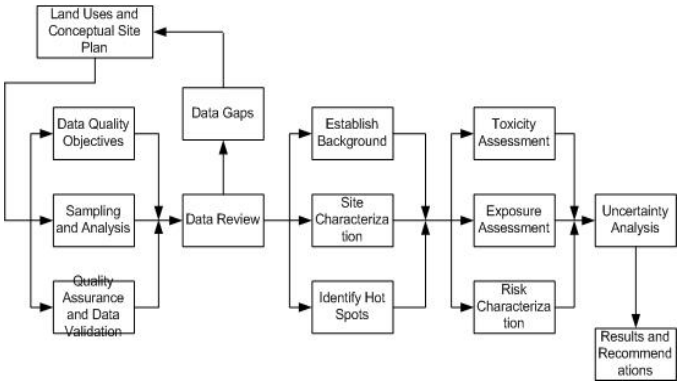

Fig. 3. Risk assessment process [43]

V. CONCLUSION

Different variants of models and multiple model complexes of natural and technological objects were reviewed and analysed in this paper. This research helps to develop a generalized description (macro-description) of various classes of natural and technological object models (macro-models) that allow, first, establishing interrelations and correspondences between the types and kinds of natural and technological object models, and, second, comparing and ranking them using various metrics. The study helps to develop combined methods for estimating quality indices of natural and technological object models (poly-model systems) given by numerical and non-numerical (nominal and ordinal) scales; to develop methods and algorithms for solving problems of multi-criteria analysis, ordering, choice of the most preferable natural and technological object models (poly-model systems), and control of their quality.

ACKNOWLEDGMENTS

The research has been supported by the project 2.1/ELRI-184/2011/14 “Integrated Intelligent Platform for Monitoring the Cross-border Natural-Technological Systems” as part of “Estonia-Latvia-Russia Cross-border Cooperation Programme within European Neighbourhood and Partnership Instrument 2007–2013”.

REFERENCES

[1] Nirupama, Slobodan P. Simonovic. Role of remote sensing in disaster management // ICLR Research. September 2002

[2] Hongcheng Zeng, Ari Talkkari, Heli Peltola, Seppo Kellomäki. A GIS-based decision support system for integrated flood management under uncertainty with two dimensional numerical simulations // Environmental Modelling& Software, Volume 22, Issue 9, September 2007, pp 1240-1249

[3] Emilio Chuvieco, Inmacula da Aguado, Marta Yebra, Héctor Nieto, Javier Salas, M. Pilar Martín, Lara Vilar, Javier Martínez, Susana Martín, Paloma Ibarra, Juan de la Riva, Jaime Baeza, Francisco Rodríguez, Juan R. Molina, Miguel A. Herrera, Ricardo Zamora. Development of a framework for fire risk assessment using remote sensing and geographic information system technologies // Ecological Modelling, Volume 221, Issue 1, 10 January 2010, pp 46-58

[4] Tuncay Kuleli, Abdulaziz Guneroglu, Fevz iKarsli, Mustafa Dihkan. Automatic detection of shoreline change on coastal Ramsar wetlands of Turkey // Ocean Engineering, Vol. 38, Iss.10, July 2011, pp 1141-1149

[5] Paolo Ciavola, Oscar Ferreira, Piet Haerens, Mark Van Koningsveld, Clara Armaroli, Quentin Lequeux. Storm impacts along European coastlines. Part 1: The joint effort of the MICORE and ConHaz Projects // Environmental Science & Policy, Volume 14, Issue 7, November 2011, pp 912-923

[6] Paolo Ciavola, Oscar Ferreira, Piet Haerens, Mark Van Koningsveld, Clara Armaroli. Storm impacts along European coastlines. Part 2: lessons learned from the MICORE project // Environmental Science & Policy, Volume 14, Issue 7, November 2011, pp 924-933

[7] Aliakbar Rasuly, Rezvan Naghdifar, Mehdi Rasoli. Monitoring of Caspian Sea Coastline Changes Using Object-Oriented Techniques // Procedia Environmental Sciences, Volume 2, 2010, pp 416-426

[8] Hongcheng Zeng, Ari Talkkari, Heli Peltola, Seppo Kellomäki. A GIS-based decision support system for risk assessment of wind damage in forest management // Environmental Modelling& Software, Volume 22, Issue 9, September 2007, pp 1240-1249

[9] David López-Carr, Jason Davis, Marta M. Jankowska, Laura Grant, Anna Carla López-Carr, Matthew Clark. Space versus place in complex human–natural systems: Spatial and multi-level models of tropical land use and cover change (LUCC) in Guatemala // Ecological Modelling, Volume 229, 24 March 2012, pp 64-75

[10] Renata Libonati, Carlos C. Da Camara, José Miguel C. Pereira, Leonardo F. Peres. On a new coordinate system for improved discrimination of vegetation and burnedareas using MIR/NIR information // Remote Sensing of Environment, Volume 115, Issue 6, 15 June 2011, pp 1464-1477

[11] Olivier Therond, Huib Hengsdijk, Eric Casellas, Daniel Wallach, Myriam Adam, Hatem Belhouchette, Roel of Oomen, Graham Russell, Frank Ewert, Jacques-Eric Bergez, Sander Janssen, Jacques Wery, Martin K. Van Ittersum. Using a cropping system model at regional scale: Low-data approaches for crop management information and model calibration // Agriculture, Ecosystems & Environment, Volume 142, Issues 1–2, July 2011, pp 85-94

[12] Wim van Leeuwen, Chuck Hutchinson, Sam Drake, Brad Doorn, Verne Kaupp, Tim Haithcoat, Vladislav Likholetov, Ed Sheffner, Dave Tralli. Benchmarking enhancements to a decision support system for global crop production assessments //Expert Systems with Applications, Volume 38, Issue 7, July 2011, pp 8054-8065

[13] Zschau J., Küppers, .A. Early warning systems for natural disaster reduction, Berlin Springer (2003), pp: 834.

[14] Zhooma P. Classifcation of technogenic landscapes// Klasyfikacja krajobrazu. Teoria i praktyka. Problemy Ekologii Krajobrazu (2008), pp 89-98.

[15] Carino N., Clifton J. Prediction of Cracking in Reinforced Concrete Structures – NISTIR 5634 (1995), pp: 51.

[16] Boris Simeonov, Experimental investigation of the strength, stiffness and ductility of RC structural Walls // World Conference on Earthquake Engineering – Vol 6 (1998), pp 387-394.

[17] Ouzaa K., Benmansour M. Cracks in base-restrained plain and reinforced concrete walls // Turkish J. Eng. Env. Sci. – Vol 34 (2010), pp 215 – 230.

[18] Cubrinovski Misko, McCahon Ian. Foundations on Deep Alluvial Soils // Technical Report Prepared for the Canterbury Earthquakes Royal Commission (2011), pp 41.

[19] Sheng-Huoo Ni, Chi-Chih Ko, Su-Yu Chen. Downhole monitoring instrumentation at Chingliao site and its monitoring data analysis // 4th International Conference on Earthquake Engineering (2006), pp 9.

[20] Sheng-Huoo Ni, Win-Gee Huang, Feng-Yi Chen. The application of AFMM aided system identification on ground vibration monitoring data analysis // The 14th World Conference on Earthquake Engineering (2008), pp: 8.

[21] Sheng-Huoo Ni, Chi-Chih Ko. Downhole monitoring instrumentation for the site liquefied during Chi-Chi earthquake at Chingliao, Tainan, Taiwan // U.S.-Taiwan Workshop on Soil Liquefaction (2003), pp 18.

[22] Kostadinov Mladen, Yamazaki Fumio. Detection of soil liquefaction from strong motion records // Earthquake engineering and structural dynamics (2001), pp. 173-193.

[23] Guide on How to Develop a Small Hydropower Plant, European Small Hydropower Association (2004), pp: 296.

[24] Calculating the amount of available power [Online] Avaliable: http://ggsingenieria.blogspot.com/2012/05/calculating-amount-of-available-power.html

[25] Close G., Lee C., Moore R. etc. Water level monitoring from space // Netherlands: European Space Agency ESA SP 458 (2000), pp.105-111.

[26] Wind Turbine Power Calculations [Online] Avaliable: http://www.raeng.org.uk/education/diploma/maths/pdf/exemplars_advanced/23_Wind_Turbine.pdf

[27] Calculations for wind energy statistics [Online] Avaliable: http://www.bwea.com/edu/calcs.html
[28] Calculating the mean power [Online] Avaliable: http://www.wind-power-program.com/mean_power_calculation.htm
[29] Viton Philip. Understanding Road Wear and its Causes // The Ohio State University, City and Regional Planning 776 Lecture Notes 2011, pp 31.
[30] Hjort Mattias, Haraldsson Mattias, Jansen Jan. Road wear from Heavy Vehicles // Report nr. 08/2008 NVF committee Vehicles and Transports (2008), pp: 47.
[31] Modelling the Marginal Cost of Road Wear // National Transport Commission (2011), pp: 60.
[32] Road Pavement Management. Discussion paper//His Majesty's government of Nepal ministry of works and transport department of roads (1995), pp: 40.
[33] B. Wisner, P. Blaikie, T. Cannon, and I. Davis. At Risk - Natural hazards, people's vulnerability and disasters, 2nd edition 2003, pp: 134.
[34] Maik Singh, Presentation on Industrial accidents, pp. 20.
[35] Measuring the Size of an Earthquake [Online] Avaliable: http://earthquake.usgs.gov/learn/topics/measure.php
[36] Report on Wind Chill Temperature and Extreme Heat Indices: Evaluation and Improvement Projects, U.S. Department of Commerce/ National Oceanic and Atmospheric Administration (2003), pp 75.
[37] Guidelines on Analysis of extremes in a changing climate in support of informed decisions for adaptation, World Meteorological Organization (2009), pp: 55.
[38] Tom De Groeve, Flood monitoring and mapping using passive microwave remote sensing in Namibia, Geomatics, Natural Hazards and Risk (2010), pp. 19-35.
[39] Flash Flood Monitoring and Prediction, Guide for Users (2007), pp. 20.
[40] Global Forest Fire Watch: Wildfire Potential, Detection, Monitoring and Assessment [Online] Avaliable: http://na.unep.net/siouxfalls/globalfire /indofire/firepaper.php
[41] Metro Graphics, Emergency Medical Services Response to Hazardous Materials Incidents, pp. 13-44
[42] Hazardous Material Emergency Response (2007), pp: 131
[43] CERCLA Baseline Risk Assessment Human Health Evaluation, U.S. Department of Energy Office of Environmental Guidance (1992), pp: 4.

Andrejs Romanovs, Dr.sc.ing., is an Associate Professor and Senior Researcher at the Institute of Information Technology, Riga Technical University. He has 25 years of professional experience teaching postgraduate courses at RTU, as well as developing more than 50 industrial and management information systems. His professional interests include modelling and design of information systems, IT governance, IT security and risk management, integrated information technologies in business, as well as education in these areas. A.Romanovs is a senior member of the IEEE, LSS; author of 2 textbooks and more than 40 papers in scientific journals and conference proceedings in the field of Information Technology.
E-mail: andrejs.romanovs@rtu.lv

Arnis Lektauers, Dr.sc.ing., is an Assistant Professor at the Department of Modelling and Simulation of Riga Technical University (RTU). His main professional interests include the development of interactive hybrid modelling and simulation algorithms with an application to complex systems analysis and the research of industrial, economic, ecological and sustainable development problems. A. Lektauers is the Secretary of Latvia Section of the Institute of Electrical and Electronics Engineers (IEEE), a member of the Council of RTU Faculty of Computer Science and Information Technology, and a member of Latvian Simulation Society, System Dynamics Society and European Social Simulation Association (ESSA). He is the author of 1 textbook and more than 30 papers in scientific journals and conference proceedings in the field of Information Technology.
E-mail: arnis.lektauers@rtu.lv

Oksana Soshko graduated from Riga Technical University (Latvia) in 2003. She holds a Master's Degree in Information Technology. Since 2003, she has been working at the Department of Modelling and Simulation of RTU. At the moment she takes a position of a Lecturer. She is a co-author of a textbook in Logistics Information Systems. Professional interests are related to information technology applications in supply chain management, as well as application of active learning methods in teaching. Oksana Soshko is an Information Coordinator of the Latvian Simulation Society.
E-mail: oksana@itl.rtu.lv

Viacheslav Zelentsov, Dr.sc. ing, is a Professor, Chief Researcher at St.Petersburg Institute of Informatics and Automation of the Russian Academy of Science, and Director of the Research and Education Centre "AeroSpaceInfo" at St.Petersburg State University of Aerospace Instrumentation. He has 35 years professional experience of educational and research activities. His professional interests include basic and applied research in integrated modelling, multi-criteria optimization under uncertainties, reliability theory, and mathematical models and methods of decision-making support in complex technical-organizational systems with the use of aerospace information. V.Zelentsov is a member of IEC, member of Doctoral Degree Granting Committee in the Bonch-Bruevich St. Petersburg State University of Telecommunications. Hi is the author of more than 250 papers in scientific journals and conference proceedings, more than 50 research and engineering projects, 5 teaching books and textbooks.
E-mail: v.a.zelentsov@gmail.com.

Andrejs Romānovs, Arnis Lektauers, Oksana Soško, Vjačeslavs Zeļencovs. Dabas un tehnoloģisko objektu monitoringa un kontroles modeļi
Dabas un sarežģītu tehnoloģisko objektu izmantošanas efektivitāti lielā mērā nosaka tas, cik mērķtiecīgi tiek veikta šīs izmantošanas vadība, kura ir iespējama, tikai izmantojot liela mēroga automatizētas vadības informācijas sistēmas. Šādu automatizētu vadības sistēmu viens no galvenajiem elementiem, kas paredzēts vadības informācijas nodrošināšanai, ir objektu stāvokļu monitoringa un kontroles sistēma. Monitoringam nepieciešamā informācija parasti tiek iegūta no dažādiem datu avotiem, tādas kā biometriskās, aerokosmiskās un citas kontroles, novērošanas un uzskaites sistēmas, un tādā veidā šāda veida informācija pēc būtības ir heterogēna (elektriskie signāli, grafiskā, tekstuālā, audio un videoinformācija utt.). Dabas un tehnoloģisko objektu monitorings ļauj novērot šo objektu izmaiņas, lai optimizētu ar dotajiem objektiem saistītos procesus, novērstu notikumus, kas var novest pie šo objektu bojājumiem; noteiktu objektu darbības ietekmes robežas; novērtētu finanšu, ekoloģiskos un citus šo objektu raksturlielumus. Ņemot vērā mūsdienu dabas un tehnoloģisko sistēmu sarežģītību un daudzfunkcionalitāti, to monitoringu ir jāveic, izmantojot liela apjoma heterogēnu datu kopas. Monitoringam un prognozēšanai tiek izmantotas dažādas metodikas un lēmumu pieņemšanas modeļi; šis raksts sniedz pārskatu par biežāk izmantotajiem dabas un tehnoloģisko objektu virszemes un kosmiskā monitoringa modeļiem, kas ir izanalizēti un izpētīti starptautiskā projekta INFROM ietvaros.

Андрей Романов, Арнис Лектауэрс, Оксана Сошко, Вячеслав Зеленцов. Модели мониторинга и контроля природных и технологических объектов
Эффективность использования природных и сложных технологических объектов во многом определяется осуществлением целенаправленного управления ими, которое возможно лишь при наличии полномасштабной автоматизированной информационной системы управления. Одним из основных элементов данной АСУ, предназначенной для информационного обеспечения управления, является система мониторинга и контроля состояний объекта. Информация для мониторинга обычно получается из различных источников данных, таких как биометрические, аэрокосмические и другие системы контроля, наблюдения и учета, и, таким образом, она является гетерогенной по своей природе (электрические сигналы, графическая, аудио, видеоинформация, тексты и т.п.). Мониторинг природных и технологических объектов позволяет наблюдать изменения в этих объектах для того, чтобы оптимизировать процессы, связанные с объектами, предотвращать события, приводящие к повреждению объектов; определить области, которые влияют на работу объекта; оценить финансовые, экологические и другие характеристики данных объектов. Принимая во внимание сложность и многофункциональность современных природно-технологических систем, их мониторинг должен производиться в условиях крупномасштабных гетерогенных наборов данных. Для мониторинга и прогнозирования используются различные методологии и модели принятия решений. Данная статья представляет собой обзор наиболее используемых моделей наземно-космического мониторинга природных и технологических объектов, проанализированных и исследованных в рамках международного проекта ИНФРОМ.